# Control of Spontaneous Emission of CdSe Nanorods in a Multirefringent Triangular Lattice Photonic Crystal

**ARTICLE** *in* JOURNAL OF PHYSICAL CHEMISTRY LETTERS · APRIL 2010

Impact Factor: 7.46 · DOI: 10.1021/jz100134y



**5 AUTHORS**, INCLUDING:

Shobha Shukla
Indian Institute of Technology Bombay
**33** PUBLICATIONS **273** CITATIONS
SEE PROFILE

Rajiv Kumar
Northeastern University
**59** PUBLICATIONS **1,983** CITATIONS
SEE PROFILE

Anderson S L Gomes
Federal University of Pernambuco
**333** PUBLICATIONS **3,731** CITATIONS
SEE PROFILE

THE JOURNAL OF PHYSICAL CHEMISTRY Letters

pubs.acs.org/JPCL

# Control of Spontaneous Emission of CdSe Nanorods in a Multirefringent Triangular Lattice Photonic Crystal

Shobha Shukla,[†,‡] Rajiv Kumar,[‡] Alexander Baev,[‡] A. S. L. Gomes,[§] and P. N. Prasad*[,†,‡,#]

[†]Department of Electrical Engineering, University at Buffalo, New York, [‡]Institute of Lasers, Photonics and Biophotonics, University at Buffalo, New York, [§]Department of Physics, Universidade Federal de Pernambuco, Recife, 50670-901 PE, Brazil, and [#]Department of Chemistry, University at Buffalo, New York

**ABSTRACT** We demonstrate dynamic control of spontaneous emission of quantum rods embedded in a large-area (~0.8 $cm^2$) triangular lattice 2D photonic crystal, which exhibits unusual multirefringence. Upon rotating the photonic crystal azimuthally, the photoluminescence of the embedded quantum rods increases abruptly at certain angles. Numerical simulations confirm that anisotropy along preferred directions, resulting in multirefringence of the crystal, is the underlying reason for the observed effect.

SECTION Electron Transport, Optical and Electronic Devices, Hard Matter

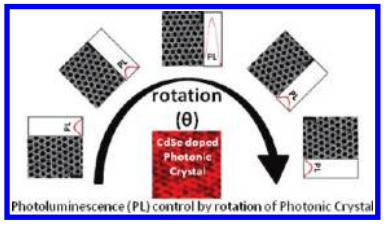


Interaction between a radiation field and matter is a fundamental phenomenon and can be controlled using photonic crystals (PhCs).[1,2] PhCs are periodic dielectric structures that affect the propagation of photons in a manner similar to that of electrons in an atomic lattice. Periodic variation of the refractive index in PhCs gives rise to guided modes, with specific dispersion of their wave vectors, and photonic band gaps. A complete band gap defines a range of frequencies for which light cannot propagate through PhCs in any direction (in-plane direction for a 2D slab). Within such a frequency range, spontaneous emission of an excited entity embedded in a PhC can be inhibited,[3−5] which has attracted a great deal of interest in the scientific community recently. This is because the ability to control spontaneous emission is of extreme importance for quantum optics and integrated photonic circuits.[6] Dynamic control of spontaneous emission can be achieved by rotating a PhC possessing anisotropic band gaps around its plane of anisotropy. Anisotropy of the photonic band gap depends on the symmetry of the crystal lattice.[7,8]

In this Letter, we report angle-dependent spontaneous emission of cadmium selenide (CdSe) quantum rods (QRs) in a large-scale, two-dimensional triangular lattice PhC. The origin of anisotropy in this case is slight disorder introduced in the crystal during the two-step fabrication process. The resulting multirefringence has been studied experimentally and theoretically in this Letter and further utilized for dynamic control of photoluminescence. Dynamic control of highly linearly polarized emission of QRs may be used for a wide range of applications.[9−15]

CdSe QRs are highly efficient, narrow line width emitters with broad spectral coverage and therefore are highly attractive as potential emitting materials for this study. To be able to control spontaneous emission of CdSe QRs, we needed a PhC with stop bands in the visible[16] range of the electromagnetic spectrum. Periodic structures can be patterned in a composite material using either e-beam lithography (EBL), two-photon absorption lithography (TPAL), or multiple beam interference lithography (MIL).[8,16] Throughput of EBL and TPAL is limited for high-volume production, especially for large-area structures. MIL, on the other hand, is an efficient way to produce 2D photonic crystals over a large area, with a precise control of the geometry and volume fraction, especially in terms of cost and time.[17]

PhCs made of composite materials not only possess enhanced lattice structure, but one can as well exploit unique properties of nanoparticles in a controlled way through periodic structures in PhCs.[15,18] Incorporation of a small amount of gold nanoparticles in SU8 helps in defining a better pattern, as reported previously.[19] The SU8 epoxy resin has good chemical and mechanical stability and has high optical transparency in the UV−vis region.[18] This makes it a good choice for patterning the PhC. A double-layer fabrication scheme was utilized for transferring the pattern to the gold-nanoparticle-doped polymer layer.[19,20]

The scanning electron micrograph of the gold-nanoparticle-doped polymer PhC, as shown in Figure 1a, reveals that the air holes acquire a well-defined circular symmetry in the PhC ($a \approx 670$ nm). The diffraction pattern from the fabricated PhC, illuminated with a 457 nm laser beam, is shown in the Figure 1a inset. Laser diffraction is an efficient and cost-effective method for characterization of large-area PhCs, as it is difficult to characterize PhCs beyond a few tens of micrometers in length with SEM. For the characterization, we have divided the 1 cm diameter PhC into four parts; the sample shown in the Figure 1a inset is of an area of 0.2 $cm^2$. The diffraction pattern consists of six equally spaced bright spots, though one bright spot is not visible in the inset of Figure 1a as

**Received Date:** February 1, 2010
**Accepted Date:** April 13, 2010
**Published on Web Date:** April 16, 2010





DOI: 10.1021/jz100134y | J. Phys. Chem. Lett. 2010, 1, 1437–1441

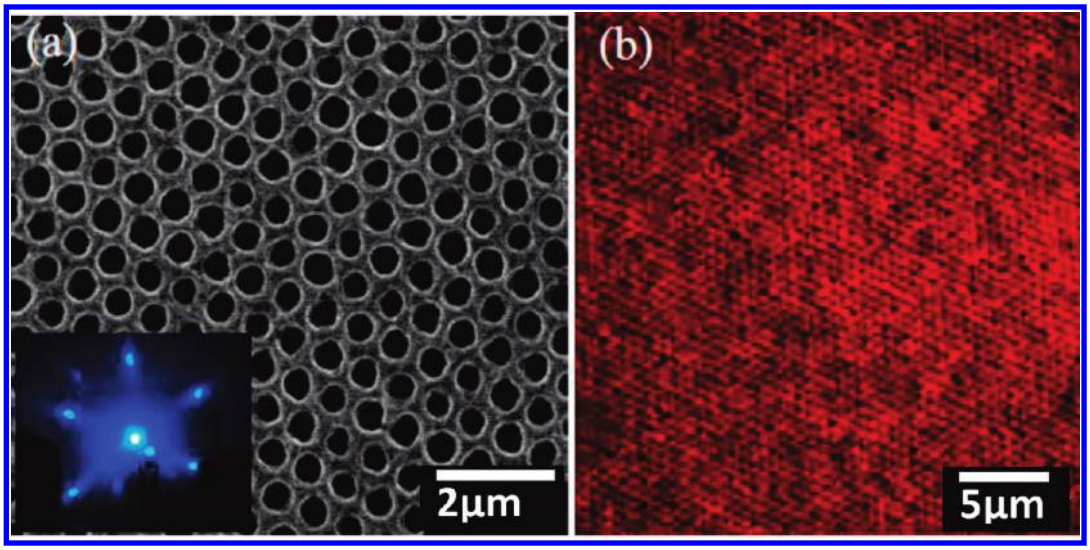


**Figure 1.** (a) Scanning electron micrograph of a gold-nanoparticle-doped SU8 PhC. The inset shows the diffraction pattern of gold-nanoparticle-doped PhC. (b) Confocal image of the QRs superlattice taken at $z = 200$ nm.

it is shadowed by the stand holding the PhC. The diffraction pattern from the triangular lattice PhC, with the regular spacing of bright spots, indicates that the pattern has hexagonal symmetry with the same crystallographic orientation throughout the whole area of the crystal.

Confocal microscopy was used to study the emission and, hence, to estimate the distribution of QRs in the PhC structure. Figure 1b shows the confocal fluorescence image of QRs in the PhC. By closely examining the confocal image, it was observed that QRs are uniformly distributed inside of the PhC. We cross-verified that QRs are deep within the air cavities of the PhC by focusing the plane of acquisition along the $z$ axis of the PhC. No fluorescence was observed from the top surface of the PhC plane.

The reflectance spectrum presented in Figure 2a clearly shows two resonant bands. The first band is centered at 1050 nm, whereas the second one is at around 550 nm. A careful investigation of the second-order band at 550 nm has revealed that the reflectance peak at around 550 nm actually consists of two resonances, one at about 530 and the second at around 570 nm. The angle-resolved reflectance spectra presented in Figure 2b show that as the sample is rotated with different values of azimuthal angle, $\varphi$, both reflectance peaks shift around, and their relative intensities change. We interpret this modification of the line profile of the reflection spectra upon rotation of the sample in accordance with the findings of Netti et al.,[21] who demonstrated optical trirefringence/multirefringence in a two-dimensional PhC slab. Mesoscale photonic patterning enables the mixing of TE and TM modes inside of the crystal, which implies that light incident with TE polarization can be reflected with TM polarization (see Supporting Information S4).[10] The polarization rotation is expected to occur along directions other than the principal axes at $\varphi = n\pi/6$ in triangular lattice structures with hexagonal symmetry. Along the principal axes though, the polarization states are pure, and in an ideal slab, two principal refractive indices are distributed between normal polarization modes. Multirefringence assumes more than two principal refractive indices. Indeed, the reflection spectra presented in Figure 2b show a strong dependence on the in-plane rotation with reference to the lattice. When the PhC was azimuthally rotated from 0 to $\pi/2$, the intensity of the 530 nm reflectance peak started to reduce with a small blue shift, and the 570 nm reflectance peak showed a red shift toward 580 nm with the rotation. At complete $\pi/2$ rotation reflectance spectra showed a very small hump at 530 nm and a distinct peak at 580 nm. When the PhC was further rotated, the 530 nm reflectance peak started to appear again and reached its normal value at full $\pi$ rotation. A few distinct refractive indices distributed between the principal axes have been identified with the angle-dependent reflectance study, $n_1(\varphi = 0, \pi)$, $n_2(\varphi = \pi/6, 7\pi/6)$, $n_3(\varphi = \pi/3, 4\pi/3)$, $n_4(\varphi = \pi/2, 3\pi/2)$, $n_5(\varphi = 2\pi/3, 5\pi/3)$, and $n_6(\varphi = 5\pi/6, 11\pi/6)$. The modification of the line profile with sample rotation can be understood in terms of the imbalance of the lattice spacings in the sample, as is observed in the scanning electron micrograph in Figure 1a. To check this hypothesis, we numerically calculated the angle-resolved reflection spectra of an ideal 2D photonic crystal slab with a triangular lattice and the lattice constant of 670 nm using the finite elements analysis.[22] The computational domain is shown in Figure 2c. All spectra were calculated with the incidence angle of 2.5° with respect to normal, corresponding to the $\Gamma$-point band edge of the slab. The azimuthal angle of 0°, $\varphi = 0$, corresponds to the $\Gamma-M$ direction within the slab. The infinite periodicity along the $x$ and $y$ axis was ensured by Floquet-type double periodic boundary conditions and periodic mesh. The reflectance spectra were normalized with respect to the spectrum of the incident wave, calculated in an identical simulation in vacuum without the slab structure. The simulated reflection spectra of unpolarized light, presented in Figure 2d, show a number of peaks; the outermost ones are at at about 520 and 565 nm. The peaks' positions reveal no dependence on in-plane rotation of the slab by $n\pi/6$ (different relative



DOI: 10.1021/jz100134y | J. Phys. Chem. Lett. 2010, 1, 1437–1441

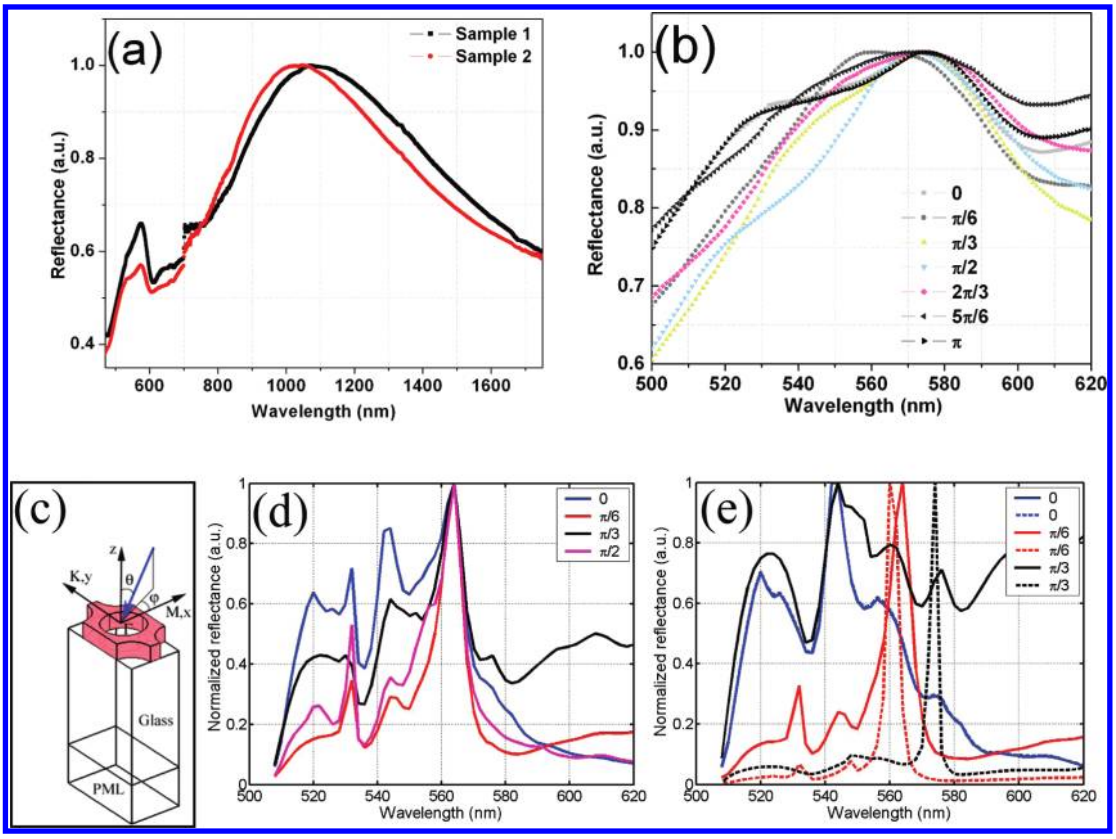


**Figure 2.** (a) Reflectance spectra of gold-doped SU8 PhCs fabricated with different exposure times. (b) Angle-resolved reflectance spectra of sample 1. (c) FEA computational domain. (d) Calculated angle-resolved reflectance spectra of PhC with lattice a constant of 670 nm. (e) Angle-resolved reflectance spectra calculated with disturbed periodicity along the $\Gamma-K$ crystallographic direction (broken curves) versus the same spectra calculated with perfect periodicity (solid curves).

intensities can be attributed to coarse meshing due to limited computational resources). This supports our hypothesis that the angular dependence of the reflection spectra of unpolarized light arises from the spatial anisotropy of the PhCs that developed during the fabrication process of a real photonic crystal. To simulate this anisotropy, we repeated the angle-resolved simulations of the reflectance spectra, using the same double periodic boundary conditions with a periodic mesh only at the boundaries perpendicular to the $\Gamma-M$ direction within the slab. The boundaries perpendicular to the $\Gamma-K$ direction were randomly meshed. At 0° and $\pi$ rotations, corresponding to only the $x$ components of the in-plane wave vector, periodicity is not disturbed. However, at $n\pi/6$ rotations, periodicity is not perfect for the $y$ components of the wave vector. Indeed, the reflectance spectra shown in Figure 2e are identical for the linearly polarized incident light with only the $x$ component of the wave vector ($\varphi = 0$). However, they differ for the linearly polarized incident light with both the the $x$ and $y$ components of the wave vector ($\varphi = \pi/6, \pi/3$).

The photoluminescence (PL) peak of colloidal CdSe QRs shown in Figure 3a is located at around 545 nm in toluene and lies within the second-order stop band of the PhC slab. It is worthwhile to note that the PL peak was a little blue-shifted inside of the PhC, as follows from comparison of PL spectra in Figure 3a and b. The absorption edge in toluene found at 430 nm lies sufficiently outside of the second-order stop band of the PhC. Hence, these colloidal nanorods form an ideal system to be studied for inhibition of spontaneous light emission in our PhC. The TEM image (inset of Figure 3a) shows the uniformity of the QRs produced. The effect of PhC anisotropy on the spontaneous emission of QRs is studied by rotation of the sample, as shown in Figure 3. We see that the PL signal increases abruptly when the sample is rotated azimuthally at $\pi/3$ and $\pi/2$, and then, it remains roughly the same for all other angles of rotation. This observation is in agreement with our reflectance study; the absence of guided in-plane modes within the stop band of the slab, manifested in higher values of reflectance, leads to a decreased PL intensity when the stop band and PL are spectrally overlapped. Modification of the spontaneous emission occurs due to redistribution of the density of photon states in the stop band.[12,23,24] Although the reflectance profiles at $\pi/3$ and $2\pi/3$ appear to be the same, close investigation reveals that at $\pi/3$, reflectance values are comparatively smaller than those at $2\pi/3$. We tentatively attribute the higher values of photoluminescence to the smaller reflectance of PhC at $\pi/3$. Since QRs are randomly oriented with respect to the elementary photonic crystal cell, the above considerations can well explain the observed angle-dependent photoluminescence of QRs embedded in the PhC slab. The observed differences in PL intensities for 0 and 180° rotation can be explained by the enhancement of



DOI: 10.1021/jz100134y | J. Phys. Chem. Lett. 2010, 1, 1437–1441

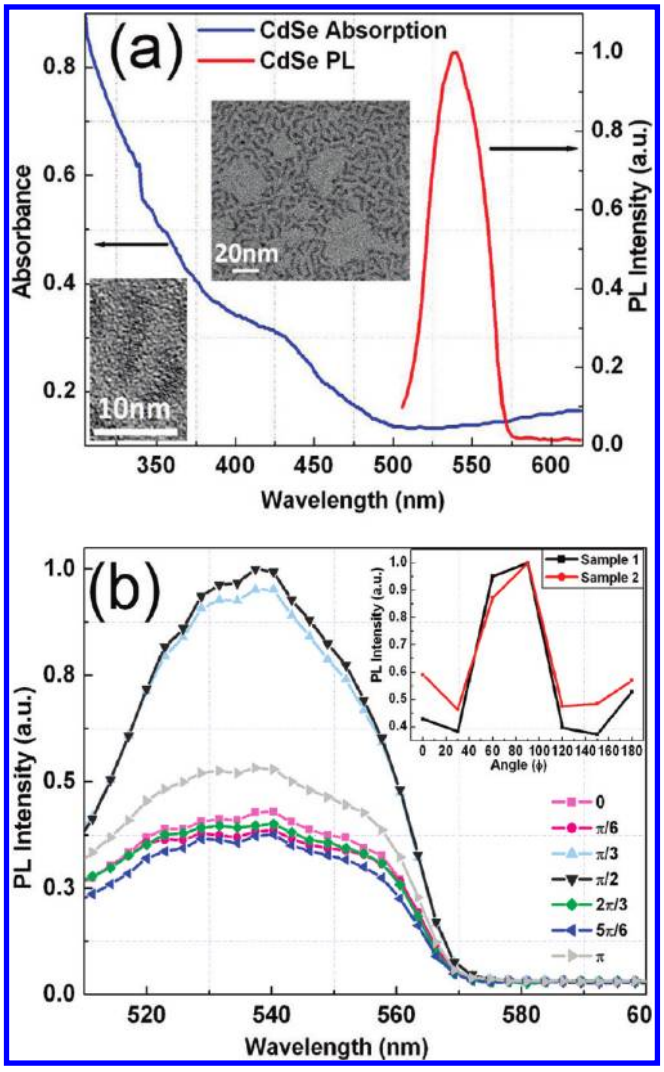


**Figure 3.** (a) Absorption and PL spectra of CdSe nanorods dispersed in toluene. The top inset shows the TEM image on the scale of 20 nm, while the lower inset shows the HRTEM images of CdSe nanorods on the scale of 10 nm. (b) Angle-resolved PL spectra from sample 1 (inset: PL versus the angle of two different samples).

photoluminescence of QRs due to photoionization and surface traps bleaching upon continuous illumination during the experiment.[24,25] Since the PL measurements were performed using a confocal microscope, where the collection angle is wider than the incidence angle, as opposed to the spectrophotometer used in the reflectance study, where incidence and collection angles were the same, a more dramatic effect on the PL intensity with PhC rotation was observed.

In this Letter, we have successfully demonstrated dynamic control of spontaneous emission from QRs embedded in a large-area (~0.8 $cm^2$) triangular lattice photonic crystal slab by simple azimuthal rotation of the slab. The photonic crystal exhibits unusual multirefringence. Upon rotating the photonic crystal azimuthally, the photoluminescence of the embedded QRs increases abruptly at certain angles. We attribute the angle-dependent enhancement/inhibition of the PL signal to the structural anisotropy of the PhC slab, developed during the fabrication process. Scanning electron microscopy images and confocal microscopy images are in good agreement with the results obtained from optical characterization of the PhC and are in qualitative agreement with the calculations using finite elements analysis. The enhancement of the PL signal of the embedded QRs was found to be repeatable in different samples produced using the described method.

## EXPERIMENTAL SECTION

A detailed description of important fabrication steps can be found in our earlier publication, and a brief description is provided in Supporting Information S1.[19] Reflectance spectra of the PhCs were measured with a Shimadzu UV−vis spectrophotometer in the wavelength range from the UV to the near-IR. The polar angle between the incident and the reflected light from the sample was set to 5°. The illuminated area for reflectance characterization was about 0.2 $cm^2$. Two samples, fabricated with different exposure times, thus having slightly different stop bands, were also measured. The QRs were prepared with hot colloidal synthesis, and a detailed procedure is given in Supporting Information S2. The QRs so prepared were incorporated into the PhC via the chemical infiltration method by soaking the PhC for 5 min in a dilute suspension of QRs in toluene. Afterward, the PhC was rinsed with isopropanol to remove the QRs from the top surface of the PhC and dried in air to ensure that the QRs were deep within the photonic crystal cavity. We expect that the infiltration fills the holes of the PhC and that, in the process of drying, the QRs distribute uniformly on the surfaces of the holes. Confocal microscopic images were obtained using a spectral confocal microscope (TCS SP2, Leica Microsystems) with a HXC PL APO CS 63.0 × 1.40 oil immersion objective. The samples were excited by a pulsed diode laser at 488 nm (PDL800-D, PicoQuant). For fluorescence acquisition from the QRs doped in the PhC, a photomultiplier tube was used with a filter of 510−600 nm. The samples were scanned for $xy\lambda$ series acquisition, and from the acquired stack profile, a localized spectrum was obtained (see Supporting Information S3 for details).

**SUPPORTING INFORMATION AVAILABLE** Fabrication of the gold-nanoparticle-doped photonic crystal, synthesis of CdSe quantum rods, and reflectance spectra of SU8−Au PhC obtained with unpolarized, s-polarized (TM), and p-polarized (TE) light. This material is available free of charge via the Internet at http://pubs.acs.org.

## AUTHOR INFORMATION

### Corresponding Author:

*To whom correspondence should be addressed. Address: Institute for Lasers, Photonics and Biophotonics 428 NSC Building, SUNY/at Buffalo Buffalo, New York 14260-3000. Website: www.photonics.buffalo.edu. Phone: 716-645-6800 ext. 2099. Fax: 716-645-6945. E-mail: pnprasad@buffalo.edu.

**ACKNOWLEDGMENT** We are thankful to Mr. Sumit Saxena, from the Department of Physics at the New Jersey Institute of Technology, for helpful suggestions and discussions. The AFOSR Grant Brazil/U.S. Physics Department UFPE and Buffalo is also acknowledged.



DOI: 10.1021/jz100134y | J. Phys. Chem. Lett. 2010, 1, 1437–1441

## REFERENCES

(1) Prasad, P. N. *Nanophotonics*; John Wiley & Sons: New York, 2004.

(2) Notomi, M. Theory of Light Propagation in Strongly Modulated Photonic Crystals: Refraction Like Behavior in the Vicinity of the Photonic Band Gap. *Phys. Rev. B* **2000,** *62*, 10696–10705.

(3) Kleppner, D. Inhibited Spontaneous Emission. *Phys. Rev. Lett.* **1981,** *47*, 233–236.

(4) Lodahl, P.; Floris van Driel, A.; Nikolaev, I. S.; Irman, A.; Overgaag, K.; Vanmaekelbergh, D.; Vos, W. L. Controlling the Dynamics of Spontaneous Emission from Quantum Dots by Photonic Crystals. *Nature* **2004,** *430*, 654–657.

(5) Vats, N.; John, S.; Busch, K. Theory of Fluorescence in Photonic Crystals. *Phys. Rev. A* **2002,** *65*, 043808–043821.

(6) Markowicz, P.; Friend, C.; Shen, Y.; Swiatkiewicz, J.; Prasad, P. N.; Toader, O.; John, S.; Boyd, R. W. Enhancement of Two-Photon Emission in Photonic Crystals. *Opt. Lett.* **2002,** *27*, 351–353.

(7) Alagappan, G.; Sun, X. W.; Yu, M. B. States of a Two-Dimensional Photonic Crystal in the Presence of Spatial Modulation and Anisotropy: A Perturbative Approach. *Phys. Rev. B* **2008,** *78*, 035112/1–035112/8.

(8) Escuti, M. J.; Crawford, G. P. Holographic Photonic Crystals. *Opt. Eng.* **2004,** *43*, 1973–1987.

(9) Masuda, H.; Matsumoto, F.; Yokoyama, S.; Mashiko, S.; Nakao, M.; Nishio, K. Lasing from Two-Dimensional Photonic Crystals Using Anodic Porous Alumina. *Adv. Mater.* **2006,** *18*, 213–216.

(10) Netti, M. C.; Harris, A.; Baumberg, J. J.; Whittaker, D. M.; Charlton, M. B. D.; Zoorob, M. E.; Parker, G. J. Optical Trirefringence in Photonic Crystal Waveguides. *Phys. Rev. Lett.* **2001,** *86*, 1526–1529.

(11) Noh, H.; Scharrer, M.; Anderson, M. A.; Chang, R. P. H.; Cao, H. Photoluminescence Modification by a High-Order Photonic Band with Abnormal Dispersion in ZnO Inverse Opal. *Phys. Rev. B* **2008,** *77*, 115136/1–115136/9.

(12) Petrov, E. P.; Bogomolov, V. N.; Kalosha, I. I.; Gaponenko, S. V. Spontaneous Emission of Organic Molecules Embedded in a Photonic Crystal. *Phys. Rev. Lett.* **1998,** *81*, 77–80.

(13) Shukla, S.; Ohulchanskyy, T. Y.; Sahoo, Y.; Samoc, M.; Thapa, R.; Cartwright, A. N.; Prasad, P. N. Polymeric Nanocomposites Involving a Physical Blend of IR Sensitive Quantum Dots and Carbon Nanotubes for Photodetection. *J. Phys. Chem. C* **2010,** *114*, 3180–3184.

(14) Masuda, H.; Yamada, M.; Matsumoto, F.; Yokoyama, S.; Mashiko, S.; Nakao, M.; Nishio, K. Lasing from Two-Dimensional Photonic Crystals Using Anodic Porous Alumina. *Adv. Mater.* **2006,** *18*, 213–216.

(15) Pompa, P. P.; Martiradonna, L; Torre, A. D.; Sala, F. D.; Manna, L.; De Vittorio, M.; Calabi, F.; Cingolani, R.; Rinaldi, R. Metal-Enhanced Fluorescence of Colloidal Nanocrystals with Nanoscale Control. *Nat. Nano.* **2006,** *1*, 126–130.

(16) Blanco, A.; Chomski, E.; Grabtchak, S.; Ibisate, M.; John, S.; Leonard, S. W.; Lopez, C.; Meseguer, F.; Miguez, H.; Mondia, J. P.; Ozin, G. A.; Toader, O.; Vandriel, H. M. Large-Scale Synthesis of a Silicon Photonic Crystal with a Complete Three-Dimensional Bandgap near 1.5 Micrometres. *Nature* **2000,** *405*, 437–440.

(17) Zhang, A. P.; He, S.; Kim, K. T.; Yoon, Y.-K.; Burzynski, R.; Samoc, M.; Prasad, P. N. Fabrication of Submicron Structures in Nanoparticle/Polymer Composite by Holographic Lithography and Reactive Ion Etching. *Appl. Phys. Lett.* **2008,** *93* (20), 203509/1–203509/3.

(18) Shukla, S.; Kim, K. T.; Yoon, Y. K.; Prasad, P. N. Plasmonic Nanoarrays Made in Porous Alumina Template. *Proc. IEEE: IEEE/LEOS Int. Conf. Opt. MEMS Nanophoton.* **2009,** 93–94.

(19) Shukla, S.; Baev, A.; Jee, H.; Hu, R.; Burzynski, R.; Yoon, Y. K.; Prasad, P. N. Large Area near Infrared (IR) Photonic Crystals with Colloidal Gold Nanoparticles Embedding. *ACS Appl. Mater. Interfaces* 2010, doi: 10.1021/am100109f.

(20) Zhang, A. P.; Burzynski, R.; Yoon, Y. K.; Prasad, P. N.; He, S. Double-Layer Fabrication Scheme for Large-Area Polymeric Photonic Crystal Membrane on Silicon Surface by Multibeam Interference Lithography. *Opt. Lett.* **2008,** *33*, 1303–1305.

(21) Netti, M. C.; Harris, A.; Baumberg, J. J.; Whittaker, D. M.; Charlton, M. B. D.; Zoorob, M. E.; Parker, G. J. Optical Trirefringence in Photonic Crystal Waveguides. *Phys. Rev. Lett.* **2001,** *86*, 1526.

(22) *COMSOL: Multiphysics Modeling and Simulation*. http://www.comsol.com/ (2010).

(23) Suzuki, T.; Yu, P. K. L. Emission Power of an Electric Dipole in the Photonic Band Structure of the fcc Lattice. *J. Opt. Soc. Am. B* **1995,** *12*, 570–582.

(24) Megens, M.; Schriemer, H. P.; Lagendijk, A.; Vos, W. L. Comment on "Spontaneous Emission of Organic Molecules Embedded in a Photonic Crystal. *Phys. Rev. Lett.* **1999,** *83*, 5401–5401.

(25) Sharma, S. C.; Murphree, J.; Chakraborty, T. Photoluminescence Spectra of Thin Films Containing CdSe/ZnS Quantum Dots Irradiated by 532-nm Laser Radiation and Gamma-Rays. *J. Lumin.* **2008,** *128*, 1771–1776.





DOI: 10.1021/jz100134y | *J. Phys. Chem. Lett.* **2010,** *1*, 1437–1441